Journal of Colloid and Interface Science **230,** 41–52 (2000)
doi:10.1006/jcis.2000.7033, available online at http://www.idealibrary.com on IDEAL®

A Light Scattering Study of the Association of Hydrophobically α- and α,ω-End-capped Poly(ethylene oxide) in Water

C. Gourier,* E. Beaudoin,* M. Duval,† D. Sarazin,† S. Maître,† and J. François,*,[1]

*Laboratoire de Physico-Chimie des Polymères, ESA 5067, UPPA/CNRS, 2 Avenue du Président Angot, 64000 Pau, France; and †Institut Charles Sadron CNRS/ULP, 6 rue Boussingault, 67083 Strasbourg cedex, France

Received September 7, 1999; accepted June 12, 2000

Several hydrophobically α- and α,ω-end-capped poly(ethylene oxide) polymers were studied by light scattering below and above their critical association concentration, in order to understand their association mechanisms. In the case of monofunctionalized PEO, a one-step closed association model well fits the experimental data, with a limit number of aggregation of about 30, consistent with other experimental data and a theoretical approach. In the case of difunctionalized PEO, a good description of the experimental data is obtained by assuming a two-step association process: at low concentration, the formation of "flower-like" micelles is well described by a closed association model, whereas at higher concentration, the progressive bridging of these "flowers" can be modeled by an open association.

Key Words: **associating polymers; light scattering; association model.**

INTRODUCTION

Among various associative polymers which have been extensively studied, hydrophobically end-capped poly(ethylene oxide)s are probably the most suitable for investigating association mechanisms (1, 2). It is possible to prepare well-defined, functionalized samples of very low polydispersity index (3–6). Moreover, characterization by viscosimetry, fluorescence, pulsed-gradient spin-echo NMR, small-angle neutron, X-ray, and light scattering can provide complementary results on their behaviors in aqueous solutions (5–10).

Association processes can be based on two models: closed association and open association (7, 11).

(i) Closed (or cooperative) association: an equilibrium between N_{ag} unimers (U) and an aggregate ($A_{N_{ag}}$) of aggregation number, N_{ag}, is considered,

$$N_{ag}U \leftrightarrows A_{N_{ag}},$$

with an association constant K_c,

$$K_c = \frac{[A_{N_{ag}}]}{[U]^{N_{ag}}}. \qquad [1]$$

The total polymer concentration C (g ml^{-1}) is related to the concentration of unimers C_u (g ml^{-1}) by

$$C = C_u\left[1 + K_c\, N_{ag}\left(\frac{1000C_u}{\overline{M_u}}\right)^{N_{ag}^{-1}}\right], \qquad [2]$$

where $\overline{M_u}$ is the weight-average molecular weight of the unimer. The weight-average molecular weight $\overline{M_w}$ of the system at a given concentration can be simply calculated according to

$$\overline{M_w} = C_u\,\overline{M_u} + (C - C_u)N_{ag}\,\overline{M_u}. \qquad [3]$$

(ii) Open (or progressive) association: successive equilibrium steps are for unimers (U) with dimers (U_2) and trimers (U_3), etc.,

$$U + U \rightleftarrows U_2$$
$$U_2 + U \rightleftarrows U_3$$
$$U_{N_{ag}-1} + U \rightleftarrows U_{N_{ag}}.$$

If the different association steps are equivalent, the system is defined by one constant association K_0:

$$K_0 = \frac{[U_{N_{ag}}]}{[U][U_{N_{ag}-1}]}. \qquad [4]$$

Elias (13) has calculated the variation of $\overline{M_w}$ for an open association model. In the case of monodisperse samples, this equation can be reduced to

$$\overline{M_w}^2 = \overline{M_u}^2 + 4000K_0C. \qquad [5]$$

In the past few years, various association mechanisms have been proposed. From light scattering measurements performed on polydisperse commercial samples of hydrophobically end-capped poly(ethylene oxide) urethanes, Maechling-Strasser *et al.* (7, 8) have concluded that the association was of the open type, but, it was difficult to know if this behavior was or was not

[1] To whom correspondence should be addressed.

0021-9797/00 $35.00

related to the sample's high polydispersity. Nyström *et al*. (9) have studied the dynamics of aqueous associative PEO solutions with dynamic light scattering and pulsed-gradient spin-echo NMR techniques. Their results indicate fractal-like structures with relaxation processes that slow down as the polymer concentration increases. From a fluorescence study, Yekta *et al*. (10) have observed that at very low concentrations, polymer associates to form micelle-like particles with an aggregation number remaining constant over a very broad concentration range where changes in solution viscosity are of several orders of magnitude. The authors have proposed a two-step mechanism involving closed association of the hydrophobic groups in micelles, and at higher concentration, open association of micelles forming aggregates responsible for the viscosity enhancement. Chassenieux *et al*. (11a) performing viscosimetric and light scattering measurements on well-defined α,ω-functionalized PEO with dodecyl end groups have also concluded that a two-step association process occurs, analogous to a system based on telechelic ionomers (11b). Sedimentation studies of Oulyanova *et al*. (12) are also in agreement with such a description. What is not clear is whether the first and second steps are open or closed.

Static light scattering (SLS) measurements provide direct information which can be used with the different association models and can lead, as shown by relations [2]–[5], to variations of $\overline{M_w}$ versus polymer concentration. Nevertheless, the difficulty in comparing predictions and experimental results arises from the existence of virial terms in SLS expressions, which are not considered in these simple models. Thus, SLS results alone are not sufficient for resolving this problem. Measurements of the aggregate size may also provide interesting information since the literature provides several theoretical calculations of static (R_g) and hydrodynamic (R_H) radii for stars, combs, and statistical branched aggregates. Moreover, fluorescence and small angle neutron scattering experiments indicate the value of the critical association concentration (*CAC*) and the average distance between micelles' centers, respectively, which can be used to test models.

Comparisons between α- and α,ω-functionalized samples is of great interest: in the first case, only the first association step is expected, which can be reasonably considered as being similar to the first association step of α,ω-functionalized samples of twice $\overline{M_u}$. Chassenieux *et al*. (11a) have studied an α-functionalized PEO with a dodecyl end group and shown that it does not associate in the concentration range explored. Therefore, no comparison between two types of polymers with the same extremity was possible.

This paper provides complementary data about the associative mechanisms of hydrophobically end-capped poly(ethylene oxide) in water over a large range of concentrations. Several samples of α- and α,ω-functionalized PEO with dodecyl and hexadecyl aliphatic end groups are investigated. The experimental study includes fluorescence, viscosity, static (SLS) and dynamic light scattering (DLS), and small-angle neutron scattering measurements (SANS). The Discussion will explain the SLS results with different association models, which must be also consistent with the results of the other measurements.

EXPERIMENTAL

α- and α,ω-end-capped PEOs were respectively prepared by chemical modification of α-(Shearwater polymers) and α,ω-hydroxylated (Hoechst) PEO. This was done by addition of an alkyl isocyanate to α- and α,ω-hydroxylated PEO in the presence of 1,4-diazobicyclo[2.2.2]octane (DABCO, Aldrich) in toluene at 30°C. The degree of functionalization was, in each case, higher than 0.95, as determined by NMR and UV spectroscopy. The polydispersity indexes were lower than 1.1 as indicated by size exclusion chromatography from a mixture of water/acetonitrile (70/30) where adsorption on columns and association do not occur (14). In this work five samples were used: M,20,18, M,20,12, D,12,12, D,20,12, and D,32,16, where the letter M or D indicates that the sample is α- or α,ω-functionalized, respectively, the first number is the molecular weight divided by 1000 (in g mol^{-1}), and the second is the number of end-group carbons.

Fluorescence was used to determine critical association concentrations *CAC*, by measuring the emission spectra of pyrene used as probe solubilized at 5×10^{-7} mol l^{-1} in polymer solutions. The spectra were recorded on a Perkin Elmer LS 50B. The ratio I_1/I_3 of the first to third peak intensities of pyrene correlates with the polarity of its immediate environment. It exhibits a strong drop from the value 1.8, generally measured in pure water or prior to polymer micellization and a much lower value (1.4–1.1, according to the system) after micellization (15–17).

Viscosity measurements were made using a low-shear viscosimeter (Contraves LS30) with a shear rate ranging from 0.01 to 128 s^{-1}, with a Couette. The system was thermostated to 25 ± 0.05°C.

Static and dynamic light scattering measurements were performed using a goniometer (Sematech) with a He–Ne laser source (wavelength $\lambda = 632$ nm). The scattering angle θ was varied between 30° and 150°. The autocorrelation function was analyzed using a SEMATECH RTG. Polymer solutions were prepared in water freshly distilled from quartz with 400 ppm sodium azide as bacteriostatic and they were stirred for at least 24 h at room temperature and filtered through 0.1 μm Dynagard filters. Occasionaly, solutions were prepared by heating at 50°C for 6 h. The concentration (C, g ml^{-1}) range varied according to the sample: for the most associative (lowest *CAC*), i.e., D,32,16, 10^{-4} g ml^{-1} $< C <$ 10^{-2} g ml^{-1} and for the least associative (highest *CAC*), i.e., D,20,12, 10^{-3} g ml^{-1} $< C <$ 10^{-1} g ml^{-1}.

SANS experiments were performed on PACE and PAXY instruments at the L. Brillouin laboratory in CEA-Saclay (France). The wavelength, λ, was set to 6 Å or 10.5 Å with respectively a sample–detector distance of 1 m and 3 m to cover a scattering vector q range between 0.006 and 0.32 Å^{-1} ($q = 4\pi/\lambda \sin(\theta/2)$, where θ is the scattering angle). Concentration was varied between 1.5×10^{-2} g ml^{-1} and 10^{-1} g ml^{-1}.

RESULTS

Fluorescence

Figure 1 reports the variations of I_1/I_3 for pyrene solubilized in aqueous solutions of α-functionalized samples, M,20,12 and M,20,18, against polymer concentration. Formation of hydrophobic microdomains is indicated by these plots and *CAC* are considered as C values when I_1/I_3 starts to drop. *CAC* is much higher for M,20,12 than for M,20,18, as expected from the differing hydrophobic group lengths.

Similar curves were published for α,ω-end-capped PEO with dodecyl end groups (5). The variation of *CAC* with the length of the PEO chain will be discussed elsewhere, in more detail. Sample D,32,16 behaves in the same manner (Fig. 6). *CAC* values for the samples under study are reported in Table 1.

Viscosity

Figure 2 shows variations of the relative viscosity η_{rel} against concentration for the associative PEO (M,20,18 and D,32,16) and the parent unmodified PEO. As frequently described in the literature, an abrupt divergence from linearity is observed at a concentration called C_η for the difunctionalized samples. More surprisingly, a lower but significant divergence is also observed for the monofunctionalized sample. C_η values I from this and previous (5) work are reported in Table 1.

In the representation of Fig. 2, no discrepancy between η_{rel} of PEO and associating samples can be observed. However, when the reduced viscosity η_{red} is plotted against C and values are extrapolated to $C = 0$, the intrinsic viscosity of M,20,18 and D,32,16 can be determined: one finds respectively $[\eta] =$ 85 ml g^{-1} and 90 ml g^{-1}, which is significantly higher than $[\eta]$ of the parent PEO (31 ml g^{-1} and 41.2 ml g^{-1}, for $\overline{M_w} = 20{,}000$ and 32,000).

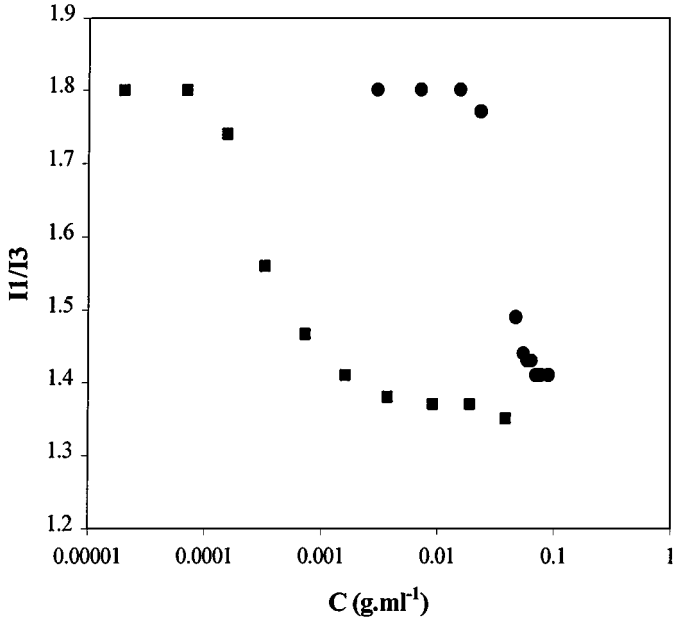

FIG. 1. Variations of the ratio I_1/I_3 against polymer concentration for aqueous solutions of M,20,10 (●) and M,20,18 (■).

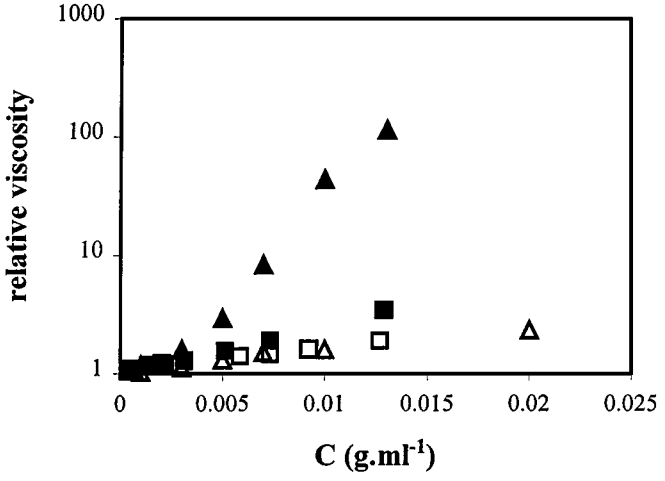

FIG. 2. Variations of the relative viscosity against concentration for associative PEO (M,20,18 (■) and D,32,16 (▲)) and the parent unmodified PEO (PEO 20 (□) and PEO 32 (△).

Light Scattering Experiments

(i) α-Functionalized PEO. DLS. In the range of concentrations investigated, 1×10^{-3} g ml^{-1} $< C < 3 \times 10^{-2}$ g ml^{-1}, DLS measurements on M,20,18 show a monomodal distribution of relaxation times, corresponding to an average hydrodynamic radius $R_H = 153 \pm 15$ Å, a value to be compared with that of the parent PEO20: $R_{HU} = 45$ Å (this last value is in good agreement with that calculated from the empirical expression of Denavand *et al.* (17), ($R_{HU} = 41$ Å). This indicates that almost

TABLE 1
Critical Concentrations for PEO and α- and α,ω-End-capped PEO Solutions

	C_p^* (g ml^{-1})	*CAC* (g ml^{-1})	C_η (g ml^{-1})	C' (g ml^{-1}) (SLS)	C'' (g ml^{-1}) (SLS)
PEO12	3.51×10^{-2}				
D,12,12		2×10^{-3}	10^{-2}	3.51×10^{-3}	1.05×10^{-2}
PEO20	2.39×10^{-2}				
M,20,12		5×10^{-2}			
M,20,18		1×10^{-4}	2×10^{-3}	$<2.4 \times 10^{-4}$	1.12×10^{-3}
D,20,12		7×10^{-3}	1.5×10^{-2}	8.36×10^{-3}	1.67×10^{-2}
PEO32	1.68×10^{-2}				
D,32,16		10^{-4}	3×10^{-3}	$<1.68 \times 10^{-4}$	3.36×10^{-3}

Note. C_p^* is the overlap concentration for unmodified PEO, *CAC* is the critical aggregation concentration obtained by fluorescence using pyrene as probe; C_η is the concentration at which the relative viscosity of functionalized PEO diverges from that of unmodified PEO; C' is the concentration at which functionalized and unfunctionalized PEO curves ($\overline{M_u}/\overline{M_{wapp}} = f(C_p/C_p^*)$) diverge from each other; C'' is the concentration at which functionalized PEO curves ($\overline{M_u}/\overline{M_{wapp}} = f(C_p/C_p^*)$, see below) start to increase again after the large decrease.

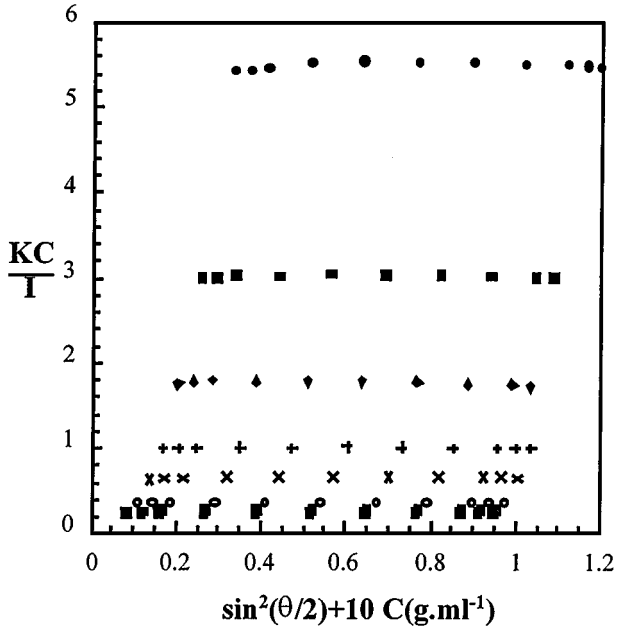

FIG. 3. Zimm plot of the sample M,20,18 in water.

only micelles are present in solution. This result is consistent with the critical association concentration (*CAC* of about 2×10^{-4} g ml^{-1}) obtained by fluorescence. The diffusion coefficient (D) increases with increasing concentration. When $C < 1.6$ g ml^{-1} the variation can be adjusted by a linear relation:

$$D = 1.5 \times 10^{-7} + 8.75 \times 10^{-6} C \ (\mathrm{cm^2\ s^{-1}}). \qquad [6]$$

Above this threshold, the variation is faster, indicating a stronger repulsion between particles.

SLS. Aqueous solutions of M,20,18 were studied in this work (10^{-3} g ml$^{-1} < C < 2.65 \times 10^{-2}$ g ml^{-1}) while sample M,20,12 was previously investigated by other authors (11a, 12). Figure 3 shows the corresponding Zimm plot, i.e., KC/I versus $\sin^2(\theta/2) + 10C$ (where K is the optical constant and I the difference of scattered intensity between solution and solvent). For small angles, KC/I is generally given by

$$\frac{KC}{I} = \left(\frac{1}{\overline{M_w}} + 2A_2C + 3A_3C^2 + \cdots\right)\left(1 + q^2\frac{R_g^2}{3}\right), \qquad [7]$$

where $q = 4\pi n/\lambda \sin(\theta/2)$, n is the refractive index of the solvent and A_2 and A_3 are the second and third virial coefficients. For associating systems, $\overline{M_w}$ is expected to be an increasing function of concentration according to relations [3] and [5].

For any C, the very small KC/I angular dependence makes an accurate evaluation of the radius of gyration R_g difficult. An order of magnitude for R_g (around 200 Å) may be given. This result is quite consistent with the above value of R_H, lower than 200 Å.

The extrapolation of KC/I to $\theta = 0$ provides variations against concentration of the $\overline{M_{wapp}}$ parameter, the so-called apparent weight-average molecular weight:

$$\left(\frac{KC}{I}\right)_{q=0} = \frac{1}{\overline{M_{wapp}}} = \frac{1}{\overline{M_w}} + 2A_2C + 3A_3C^2 + \cdots. \qquad [8]$$

Although it represents both thermodynamic and molecular weight contributions, this parameter is currently used. If virial terms were zero, it should be equal to $\overline{M_w}$. Figure 4 shows the evolution of $\overline{M_{wapp}}$ with C.

For the lowest concentration studied ($C = 4.78 \times 10^{-4}$ g ml^{-1}), the value of $\overline{M_{wapp}} = 2.5 \times 10^5$ g mol^{-1} is higher than that of the unimer $\overline{M_u} = 2 \times 10^4$ g mol^{-1}. Again, this result is consistent with a small *CAC* value (2×10^{-4} g ml^{-1}). As polymer concentration increases, $\overline{M_{wapp}}$ increases and passes through a maximum (2.9×10^5 g mol^{-1} for $C = 1.12 \times 10^{-3}$ g ml^{-1}) and then sharply decreases, attaining values lower than $\overline{M_u}$. This behavior is typical of the formation of strongly repulsive particles, whose molecular weight increases with increasing concentration. As C increases, the first term of Eq. [7] decreases while the following two increase if A_2 and A_3 are positive, leading to a maximum. The maximum value of M_{wapp} indicates that the aggregation number of the micelles is at least $\overline{M_{wapp}}/\overline{M_u} = 15$.

It is interesting to compare these results with those obtained for pure PEO according to a representation suggested by Chassenieux *et al.* (11a) (see Fig. 5). For unmodified PEO in water, the normalized curve $(KC/I)/\overline{M_u} = \overline{M_u}/\overline{M_{wapp}}$ versus C/C^* (where C^* is the critical overlap concentration for PEO:

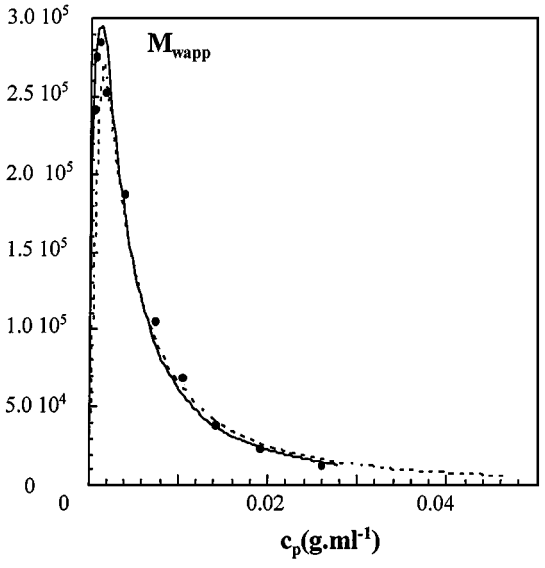

FIG. 4. Evolution of the apparent molecular weight of sample M,20,18 with concentration (●). The lines indicate variations of apparent molecular weight ($\overline{M_{wapp}}$) for two sets of adjustable parameters: closed association model (---) $N_{ag} = 30$, $K_c = 10^{135}$ g^{29} mol^{-29}, $2A_2 = 8 \times 10^{-4}$ ml mol g^{-2}, $3A_3 = 0.055$ ml^2 mol g^{-3}; open association model (—) $K_0 = 10^{6.35}$ mol g^{-1}, $2A_2 = 9 \times 10^{-4}$ ml mol g^{-2}, $3A_3 = 0.064$ ml^2 mol g^{-3}.

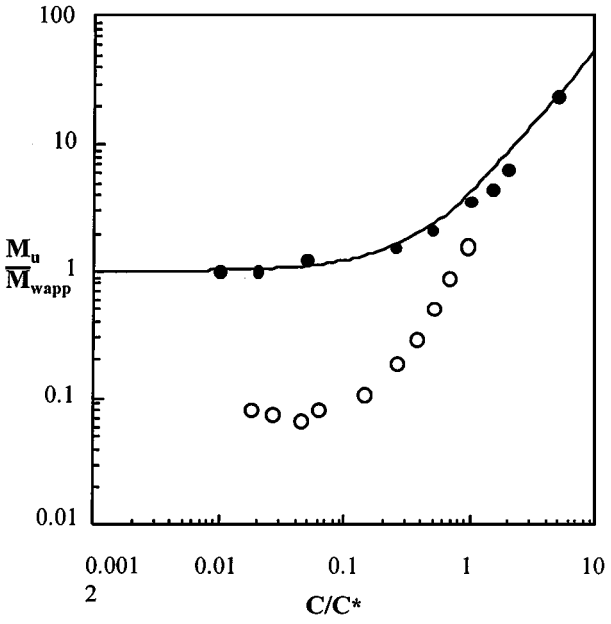

FIG. 5. Comparison of the variation of $\overline{M_u}/\overline{M_{wapp}}$ with C/C^* for unmodified PEO (—) and for M,20,12 (Ref. 11, ●) and M,20,18 (this work, ○) samples.

$C^* = \overline{M_u}/(4/3)\pi N_a R_g^3$, calculated from the experimental data of Ref. 14) is independent of the polymer molecular weight (15). The solid line in Fig. 5 shows this universal curve for PEO. While Chassenieux *et al*. (11a) have observed the same behavior as that of PEO for the sample M,20,12 (Fig. 5), the results obtained for M,20,18 are completely different. From the lowest concentration explored ($C = 4.78 \times 10^{-4}$ g ml^{-1}), the $(KC/I)/\overline{M_u}$ curve for M,20,18 is below that of PEO. This indicates the great influence of end group length.

(ii) α,ω-Functionalized PEO. DLS. Previous work performed on D20,12 and D,12,12 has shown that time-correlated functions are far from single exponentials (11a, 19). Nevertheless, the existence of a very slow mode (corresponding to $R_H > 500$ Å) was attributed to spurious aggregates which are also present in pure PEO solutions. For $C < CAC$, the fast mode corresponds to unassociated unimers and at $C \approx CAC$, a shift is observed toward higher relaxation times, which indicates micellization. At higher concentrations, the diffusion coefficient increases again, due to repulsion between particles.

For D,32,16, only one relaxation time was observed in the range of concentrations explored (10^{-4} g ml$^{-1} < C < 8 \times 10^{-3}$ g ml^{-1}). For $C < 6 \times 10^{-4}$ g ml^{-1}, it corresponds to $R_H = 150$ Å and for $C > 1 \times 10^{-3}$ g ml^{-1}, D decreases strongly (Fig. 6). Unfortunately, measurements are missing for $C > 1 \times 10^{-2}$ g ml^{-1}, but we assume that D increases again. Thus, DLS shows at first the behavior of isolated "flowers" and in a second step "flower" association.

SLS. Behaviors of several α,ω-functionalized PEOs are shown in Fig. 7, with normalized coordinates. At lower concentrations, the curves are superimposed with that of pure PEO for D,12,12 and D,20,12. For higher concentrations, $(KC/I)/\overline{M_u}$ decreases strongly and increases again to join the reference curve. The same curves features were already published for diblock copolymers (20, 21). For D,32,16 solutions, in the whole range of concentrations studied, $\overline{M_{wapp}}$ values are always much higher than that of the unmodified PEO. Again, the importance of the end group length is highlighted and this result is consistent with DLS and fluorescence measurements. Starting from this representation, and to generalize the results obtained with α- and α,ω-functionalized PEO (Figs. 5 and 7), two critical concentrations could be defined:

- C', the concentration where the $(\overline{M_u}/\overline{M_{wapp}} = f(C/C^*))$ curve of modified PEO diverges from that of unmodified PEO;
- C'', the concentration where the modified PEO curves exhibit a minimum.

Values of C' and C'' are reported in Table 1 and can be compared with CAC, C_η, and C^*.

For M,20,18 and D,32,16 it was not possible to obtain good light scattering results at concentrations lower than CAC; thus, exact values of C' cannot be given. For PEO modified with dodecyl groups, $\overline{M_u}/\overline{M_{wapp}} = f(C/C^*)$ is a powerful representation to evaluate CAC through the C' value. C' shifts toward small values when $\overline{M_u}$ increases, which is consistent with better associativity of shorter PEO. The difference observed for D,12,12 between previous (11a) and this work is probably due to the absence of spurious aggregates here as samples came from the same reaction (made in our laboratory) in both cases. Values of C' deduced from Fig. 7 however are in good agreement with the fluorescence data (Table 1). It is thus consistent to assume the same meaning for CAC and C'.

Table 1 shows that C'' values are always very close to C_η and the same meaning for C'' and C_η can be assumed.

Such a correlation between critical concentrations obtained from various experiments is clearly confirmed in Fig. 6 where variations of $\overline{M_{wapp}} = I/KC$, I_1/I_3, and η_{rel} are compared for sample D,32,16. One may also distinguish two concentration regimes in the I/KC curve in the range between C' and C''. Below a third concentration C''', the increase in this parameter is much lower than for $C''' < C < C''$. Interestingly, C''' corresponds to an abrupt jump of R_H as obtained by DLS (Fig. 6). These results are in agreement with those of Ref. (22).

For M,20,12 solutions, C'' is around C^*, whereas it is much smaller (around $0.1C^*$) for the more associative M,20,18, D,32,16, and D,12,12.

Small-Angle Neutron Scattering Experiments (SANS)

We have already shown that neutron scattering curves of α,ω-functionalized PEO in a mixture of H_2O/D_2O (82.4/17.6) (where the PEO chains are matched) always exhibit at least one broad peak at small q values and a second one which appears as a shoulder at higher q (5, 6) indicating a liquid-like order. With changing temperature, concentration and molecular weight, diffraction patterns are characteristic of a micellar

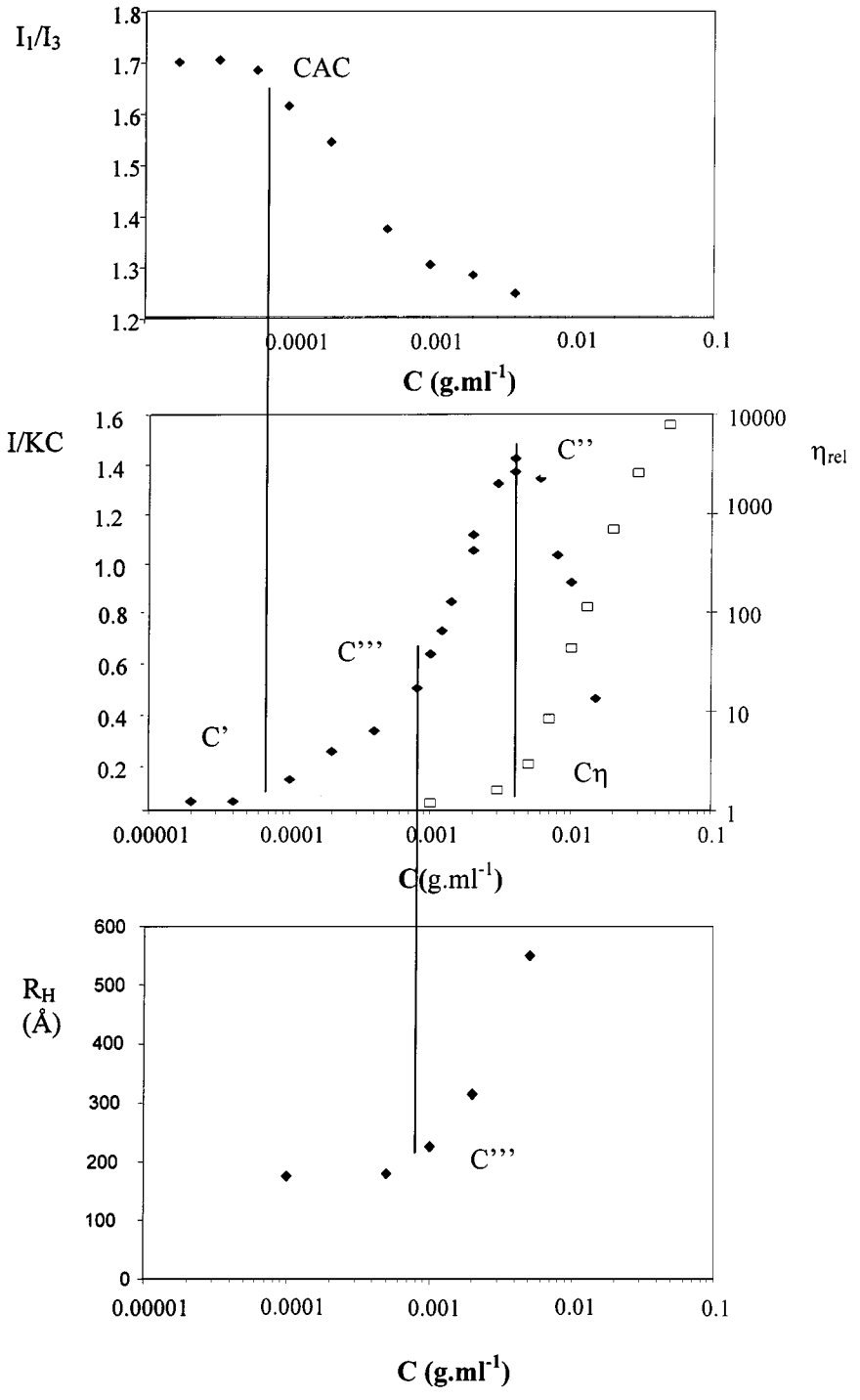

FIG. 6. Different critical concentrations for D,32,16 determined by fluorescence, SLS, viscosity and DLS.

cubic phase (six well-defined peaks), and we have concluded that these curves indicate a local cubic order.

In pure D_2O, one small-angle peak is observed in the scattering curve, at the same q value as for the matching mixture. This behavior shows that polymer–polymer interactions are different for modified PEO solutions and unmodified PEO solutions, the latter exhibiting a classical decrease of I when q increases (23–25). For the samples investigated here, this peak becomes significant for concentrations above 1–2%; its intensity passes through a maximum, to vanish at around 30–40%. This behavior is due to the strong overlap of PEO micelle corona (14, 26). These results will be detailed elsewhere.

Solutions of M,20,18 and M,20,12 have also been studied in heavy water by small-angle neutron scattering (Fig. 8) and the

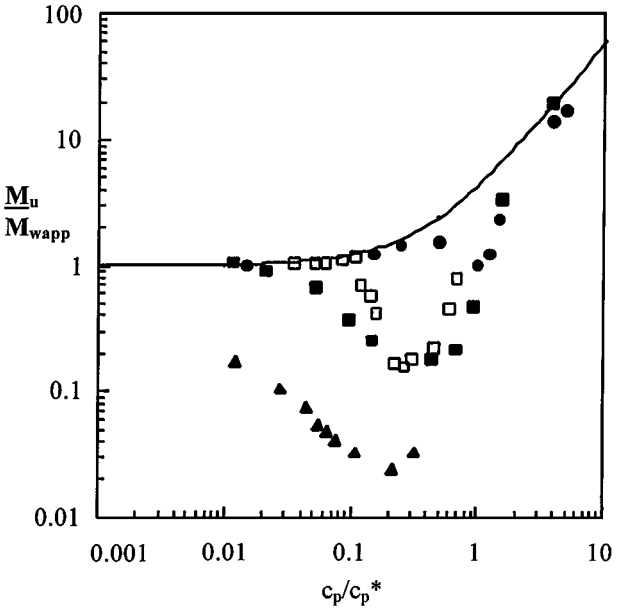

FIG. 7. Comparison of the variation of $\overline{M_u}/\overline{M_{wapp}}$ with C/C^* for unmodified PEO (—) and for D,12,12 (this work, □; Ref. 11a, ■), D,20,12 (●), and D,32,16 (▲) samples.

scattered intensity function exhibits a well-defined peak as seen for α,ω-functionalized PEO.

In all cases of α- and α,ω-functionalized PEO, the position of the peak q_{max} varies as C^a with a close to 1/3. This result indicates that the aggregation number remains almost constant, in agreement with the conclusions of Ref. (10). Assuming a

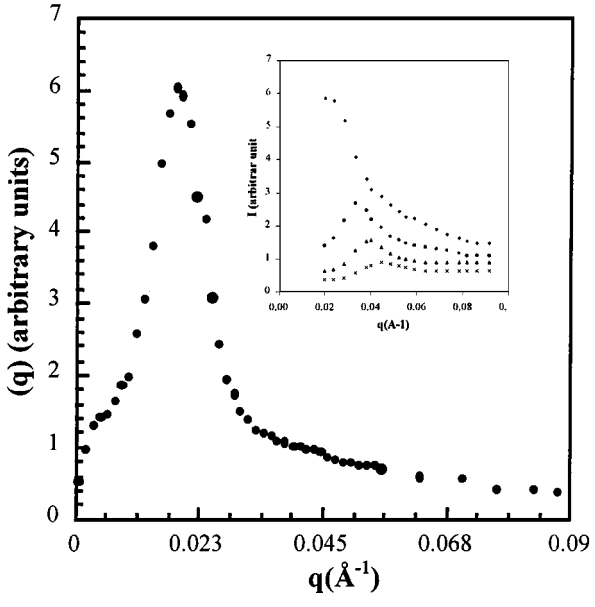

FIG. 8. Small-angle neutron scattering curve of an M,20,18 solution at $C = 5 \times 10^{-2}$ g ml^{-1}. Inset: M,20,12 solution at (◆) $C = 5 \times 10^{-2}$ g ml^{-1}, (●) $C = 11.32 \times 10^{-2}$ g ml^{-1}, (△) $C = 18.17 \times 10^{-2}$ g ml^{-1}, and (×) $C = 27.33 \times 10^{-2}$ g ml^{-1}.

TABLE 2

Average Distance $d = 2\pi/q_{max}$ between Scattering Centers in SANS Experiments at $C = 5 \times 10^{-2}$ g ml^{-1} and Aggregation Numbers Deduced from These Values

	d (Å)	N_{ag}
M,20,18	288	33
D,12,12	196	19
D,32,16	264	17

simple cubic structure, an average value of N_{ag} can be deduced from q_{max} according to

$$N_{ag} = \left(\frac{2\pi}{q_{max}}\right)^3 \frac{C N_a}{\overline{M_u}} \times 10^{-24}, \qquad [9]$$

where q_{max} is expressed in Å^{-1} and C in g ml^{-1} and N_a is the Avogadro number. In this expression, the average distance d between the centers of the micelles is assumed to be equal to $2\pi/q_{max}$. Table 2 gathers values of d and N_{ag}.

DISCUSSION

α-Functionalized PEO

In the case of M,20,18, a suitable association model must respect the following experimental results:

(1) $N_{ag} \geq 15$ at $C = 1.2 \times 10^{-3}$ g ml^{-1} (maximum of $\overline{M_{wapp}} = f(C)$);
(2) $CAC = 2 \times 10^{-4}$ g ml^{-1} (fluorescence);
(3) $N_{ag} \approx 33$ at $C = 5 \times 10^{-2}$ g ml^{-1} (SANS);
(4) $R_H \approx 3.4$ times higher than R_{HU} (DLS).

For a closed association model (Eqs. [2], [3], and [8]), the best fit of SLS measurements was obtained with $N_{ag} = 30$, $K_c = 10^{134} g^{(N_{ag}-1)}$ mol$^{-(N_{ag}-1)}$, $2A_2 = 8 \times 10^{-4}$ ml mol g^{-2}, and $3A_3 = 0.055$ ml^2 mol g^{-3} (Fig. 4). This is in good agrement with results from SANS, but the *CAC* value calculated with these parameters (4×10^{-4} g ml^{-1}) is slightly higher than the experimental value, 2×10^{-4} g ml^{-1}, obtained by fluorescence.

Open association can also lead to a good fit with $K_0 = 10^{6.35}$ mol g^{-1}, $2A_2 = 9 \times 10^{-4}$ ml mol g^{-2}, and $3A_3 = 0.064$ ml^2 mol g^{-3} (Fig. 4), by respecting condition 1. Figure 9 shows that for $C > 3 \times 10^{-3}$ g ml^{-1}, $\overline{M_w}$ increases above 6×10^5 ($N_{ag} = 30$) and attains 2×10^6, at 2%, which is not compatible with SANS experiments.

Closed association can be considered a good model, with $N_{ag} \approx 30$ but, in addition, condition 4 must be respected. To verify this, we have assumed that M,20,18 micelles are similar to polymer stars of N_{ag} branches and have used theoretical expressions giving the ratio h of the hydrodynamic radius of a star R_{HS} and that of the linear polymer of the same molecular weight

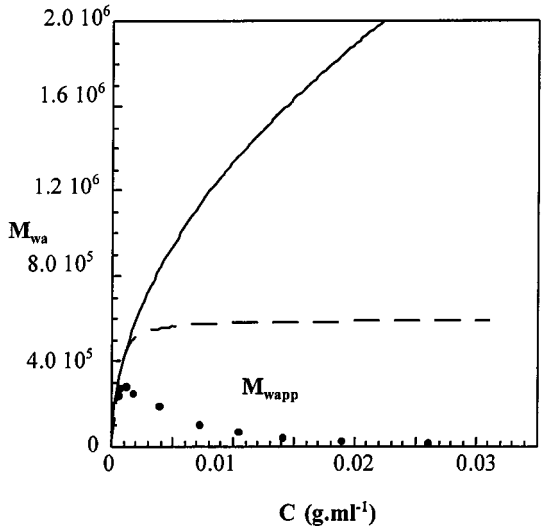

FIG. 9. Comparison between the values of the apparent molecular weight $\overline{M_{\text{wapp}}}$ deduced from light scattering experiments and the values of the weight-average molecular weight $\overline{M_{\text{w}}}$ calculated with the models of closed ((––), $N_{\text{ag}} = 30$) and open association (—) for the M,20,18 solution. The fit parameters were given in Fig. 4.

$\overline{M_{\text{WL}}}(R_{\text{HL}})$, for regular stars (27),

$$h = \frac{R_{\text{HS}}}{R_{\text{HL}}} = \frac{\sqrt{N_{\text{ag}}}}{(2 - N_{\text{ag}}) + \sqrt{2}(N_{\text{ag}} - 1)}, \qquad [10]$$

or for polydisperse stars (28),

$$h = \frac{16}{3(N_{\text{ag}} + 3)} = \left(\frac{N_{\text{ag}} + 1}{\pi}\right)^{0.5}. \qquad [11]$$

Using the power law proposed by Denavand and Selser (18), i.e.,

$$R_{\text{HL}} \propto \overline{M_{\text{wL}}}^{0.571}, \qquad [12]$$

one finds

$$h' = \frac{R_{\text{HS}}}{R_{\text{HU}}} = h(N_{\text{ag}})^{0.571}. \qquad [13]$$

For $N_{\text{ag}} = 30$, h' values are 3 and 3.5 for regular and polydisperse stars, respectively. The second result is in good agreement with the experimental value of $h' = 3.4$ but there is an inconsistency with the closed model which corresponds to monodisperse micelles. On the other hand, the value 3 for regular stars is underestimated by the calculation because the micelles' cores are not punctual but can be considered as spheres of non-negligible volume (radius of 15 Å for $N_{\text{ag}} = 30$).

Even if a closed association model is satisfactory for this α-functionalized sample, it is still approximate and it is interesting to compare it with more elaborate approaches. From arguments developed by Tanford (29) for low-molecular-weight surfactants Alami *et al*. (19) have proposed a model, that we call "modified open association" (MOA), where the micellization free energy per unimer can be expressed by

$$\frac{\Delta G_0}{RT} = -B_0 + B_1 N_{\text{ag}}^{-1/3} + B_2 N_{\text{ag}}^{1/2} \ln \frac{\overline{M_{\text{u}}}}{M_0}. \qquad [14]$$

$\overline{M_{\text{u}}}/M_0 = j$ is the polymerization degree of the PEO chain. The two first terms correspond to the hydrophobic group contribution and the third one, derived from the theories of Semenov *et al*. (30), corresponds to that of the PEO corona. The mole fraction of micelles of N_{ag} unimers, $x_{N_{\text{ag}}}$, is related to the mole fraction of unimers, x_1, by

$$x_{N_{\text{ag}}} = x_1^{N_{\text{ag}}} \exp\left(-\frac{N_{\text{ag}} \Delta G_0}{RT}\right). \qquad [15]$$

The variations of

$$\overline{M_{\text{w}}} = \overline{M_{\text{u}}} \frac{\sum_1^\infty x_{N_{\text{ag}}} N_{\text{ag}}^2}{\sum_1^\infty x_{N_{\text{ag}}} N_{\text{ag}}} \qquad [16]$$

against

$$C = \frac{55 \overline{M_{\text{u}}}}{1000} \sum_1^\infty x_{N_{\text{ag}}} \qquad [17]$$

are easily obtained, if the constants B_0, B_1, and B_2 are known. Their values were determined by considering that $\overline{M_{\text{w}}}$ starts to increase when $C = CAC$, given by fluorescence and using the known free energy contribution of each CH_3 (2200 cal mol^{-1}) and CH_2 (850 cal mol^{-1}) group (29, 31). The sets of values which give a good account for the values of *CAC* of monofunctionalized samples are

C_{18}, $j = 454$ (M,20,18) $\quad B_0 = 30.3 \quad B_1 = 30 \quad B_2 = 0.17$

C_{12}, $j = 454$ (M,20,12) $\quad B_0 = 24.3 \quad B_1 = 27 \quad B_2 = 0.17$.

In Fig. 10, the results obtained for closed association and MOA are compared for M,20,18. Both models give a good account of *CAC* and final molecular weight, but in an intermediate concentration range, $\overline{M_{\text{w}}}$ increases more quickly than in the closed model. However, the differences are small and it is difficult to measure them. Finally, the MOA model is in fact very close to the closed model and we consider only the second one for the interpretation of results obtained on α,ω-functionalized PEO. For both models, polydispersity is very low when $C \gg CAC$, but in the vicinity of *CAC*, MOA leads to a much broader polydispersity. This may explain the closer agreement of the R_{H} experimental value with those calculated for polydisperse rather than regular stars.

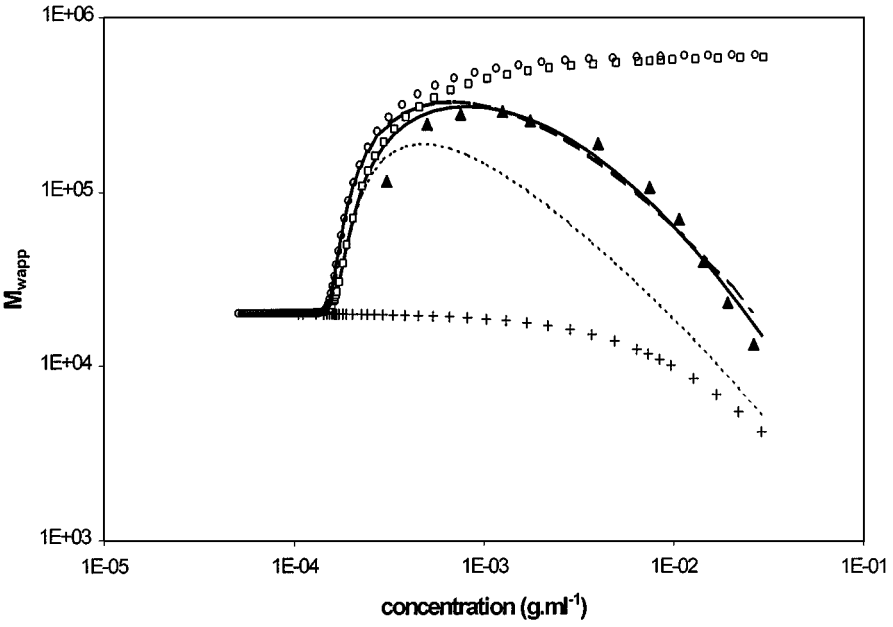

FIG. 10. Values of $\overline{M_w}$ for M,20,18 calculated with the models of closed (○) and modified open association (MOA) (□). Fit of the experimental $\overline{M_{wapp}} = f(C)$ curve of M,20,18 water solution (▲) with closed association model (–––); MOA with $2A_2 = 1 \times 10^{-3}$ ml mol g^{-2} and $3A_3 = 4.5 \times 10^{-2}$ ml^2 mol g^{-3} (best fit) (—); MOA with $2A_2 = 4.6 \times 10^{-3}$ ml mol g^{-2} and $3A_3 = 7 \times 10^{-2}$ ml^2 mol g^{-3} (values for pure PEO) (----); and calculated $\overline{M_{wapp}} = f(C)$ curve for pure PEO 20000 (+).

Remarks

In this work, A_2 and A_3 values are adjusted and in the absence of any complementary results (DLS, fluorescence, and SANS), the number of possible sets of suitable parameters should be huge. To avoid this problem, Chassenieux *et al.* (11a) have assumed that virial coefficient values are the same for modified and unmodified polymers. In our opinion, this assumption is incorrect as small-angle neutron scattering experiments performed on α-functionalized PEO solutions have revealed a correlation peak characteristic of liquid order (Fig. 8).

On the other hand, values of A_2 and A_3 used to get good fits for M,20,18 are respectively 5 and 2 times lower than those corresponding to pure PEO in water ($2A_2 = 4.6 \times 10^{-3}$ ml mol g^{-2}, $3A_3 = 7 \times 10^{-2}$ ml^2 mol g^{-3}). This indicates that at low concentrations, molecules of associative polymers are less repulsive than PEO molecules, due to the presence of hydrophobic groups. After micellization, repulsion between PEO corona occurs, and as seen in Fig. 10, values of $\overline{M_{wapp}}$ or I/KC coincide again at high concentrations for modified and unmodified PEO.

From the curve of Fig. 2, the intrinsic viscosity of M,20,18 can be calculated, and one finds $[\eta] = 85 \pm 5$ ml g^{-1}. Retaining a good measurement accuracy, the lowest concentration was 1×10^{-3} g ml^{-1}, where unimer concentration is negligible (remaining close to $CAC = 1 \times 10^{-4}$ g ml^{-1}). One can consider that the extrapolation of reduced viscosity to $C = 0$ represents $[\eta]$ of micelles. Zimm and Stockmayer (32, 33) have defined a parameter g as the ratio

$$g = \frac{R_{gS}^2}{R_{gL}^2} = \frac{3N_{ag} - 2}{N_{ag}^2}, \qquad [18]$$

where respectively R_{gS} and R_{gL} are the square average radii of gyration for a star of N_{ag} branches and for the equivalent linear polymer of the same molecular weight. Taking into account the competing effects of branching and hydrodynamic interactions, Zimm and Kilb (34) calculated the ratio of star and linear chain viscosities as $g^{1/2}$, which leads to

$$l = \frac{[\eta]_s}{[\eta]_u} = g^{1/2} N_{ag}^{0.64}, \qquad [19]$$

where indices s and u refer to micelles and unimers, respectively. Using the power law given by Louai *et al.* (35), $[\eta]_u \propto M^{0.64}$ for pure PEO, a value of $l = 2.75$ is found with $N_{ag} = 30$, which corresponds to $[\eta]_s = 90$ ml g^{-1}. Such a good agreement between theoretical and experimental values is probably fortuitous but does indicate the self-consistency of these results.

From this value of $[\eta]$, a first divergence of viscosity from linear behavior is expected for $C_m^* = 1/[\eta] = 1.2 \times 10^{-2}$ g ml^{-1}, close to the experimental value $C_\eta = 2 \times 10^{-2}$ g ml^{-1}. Nevertheless, at higher concentration, around 4×10^{-2} g ml^{-1}, an abrupt jump of almost 2 orders of magnitude in reduced viscosity is observed, a phenomenon which will be discussed elsewhere.

α,ω-Functionalized PEO

The SLS results will be discussed using the same method as above, taking into account fluorescence, viscosity, DLS, and neutron scattering results. The main difference between mono- and difunctionalized PEO is that the former can show intermicellar bridging at or before overlap concentration of flowers. One can imagine either a unique step association model (as for

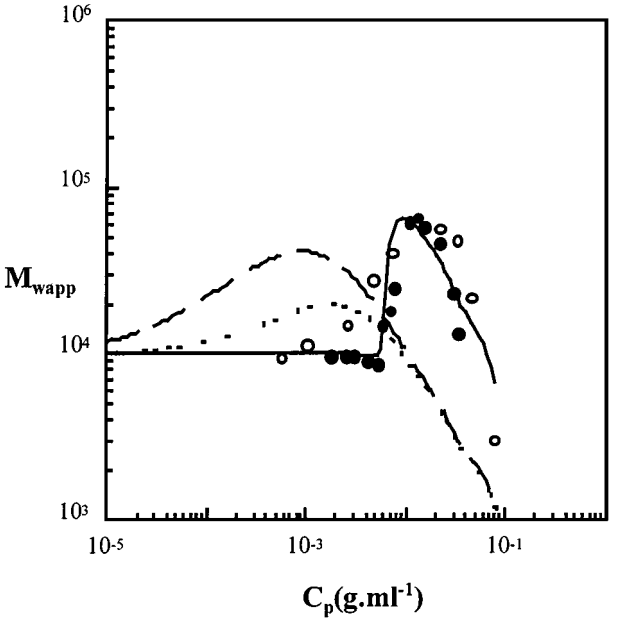

FIG. 11. Fit of the experimental $\overline{M_{\text{wapp}}} = f(C)$ curve of D,12,12 water solution (○, Ref. 12; ●, this work) with a one-step association model: (—) closed association model, $N_{\text{ag}} = 55$, with $K_{\text{c}} = 10^{170}$, $2A_2 = 1 \times 10^{-3}$ ml mol g^{-2}, and $3A_3 = 3.7 \times 10^{-2}$ ml^2 mol g^{-3}; (- - -) and (– –) open association model) with respectively $K_0 = 10^{10}$ and $K_0 = 10^9$.

α-functionalized PEO solutions) or, more likely, a two-step association model, the first forming flower-like micelles, and the second bridging these flowers.

(i) One-step association model. Figure 11 shows that the $\overline{M_{\text{wapp}}} = f(C)$ variation obtained with sample D,12,12 can be well adjusted by a one-step model of closed association with $N_{\text{ag}} = 55$, while the best fit obtained with a model of open association cannot give a good account of the results. However, the value $N_{\text{ag}} = 55$ is high compared with that deduced from neutron scattering measurements ($N_{\text{ag}} = 19$).

As expected, a unique step association process cannot correctly describe both flower-like formation and intermicellar bridging.

(ii) Two-step association models. Two steps of open association are similar to one open association; therefore only two situations have to be considered:

—Two successive closed associations according to

$$N_{\text{ag}}U \overset{K_{\text{c}}}{\rightleftarrows} A_{N_{\text{ag}}}$$
$$JA_{N_{\text{ag}}} \overset{K_{\text{c2}}}{\rightleftarrows} A_{JN_{\text{ag}}}$$

where $A_{JN_{\text{ag}}}$ is the aggregate formed by association of J flowers through intermicellar bridges. Such a model introduces two new adjustable parameters: a second constant $K_{\text{c}_2} = [A_{JN_{\text{ag}}}]/[A_{N_{\text{ag}}}]^J$ and J. One can calculate the weight-average molecular weight $\overline{M_{\text{w}}}$ of the system and the different unimer concentrations: C_{u} (free unimers), C_N (unimers in micelles) and C_{NJ} (unimers in aggregates):

$$C_{\text{u}} = C - (C_N + C_{NJ}), \quad [20]$$

$$C_N = K_{\text{c}} N_{\text{ag}} (1000)^{(N_{\text{ag}}-1)} \overline{M_{\text{u}}}^{(1-N_{\text{ag}})} C_{\text{u}}^{N_{\text{ag}}} \quad [21]$$

$$C_{NJ} = K_{\text{c}2} J 1000^{(J-1)} N_{\text{ag}}^{(1-J)} \overline{M_{\text{u}}}^{(1-J)} C_N^J \quad [22]$$

$$\overline{M_{\text{w}}} = \frac{C_{\text{u}} + C_N N_{\text{ag}} + C_{NJ} N_{\text{ag}}}{C} \overline{M_{\text{u}}}. \quad [23]$$

—A closed association (formation of "flowers") followed by an open association (flower bridging) according to

$$N_{\text{ag}}U \overset{K_{\text{c}}}{\rightleftarrows} A_{N_{\text{ag}}}$$
$$2A_{N_{\text{ag}}} \overset{K_0}{\rightleftarrows} A_{2N_{\text{ag}}}$$
$$A_{N_{\text{ag}}} + A_{2N_{\text{ag}}} \rightleftarrows A_{3N_{\text{ag}}}$$
$$A_{N_{\text{ag}}} + A_{(J-1)N_{\text{ag}}} \rightleftarrows A_{JN_{\text{ag}}}.$$

Constants K_{c} and K_0 are assumed to be:

$$K_{\text{c}} = \frac{[A_{N_{\text{ag}}}]}{[U]^{N_{\text{ag}}}} \quad [24]$$

$$K_0 = \frac{[A_{JN_{\text{ag}}}]}{[A_{N_{\text{ag}}}][A_{(J-1)N_{\text{ag}}}]} \quad [25]$$

and

$$C_{NJ} = J K_0^{(J-1)} (1000)^{(J-1)} N_{\text{ag}}^{(1-J)} \overline{M_{\text{u}}}^{(1-J)} C_N^J \quad [26]$$

$$\overline{M_{\text{w}}} = \frac{C_{\text{u}} + C_N N_{\text{ag}} + \sum_2^J J C_{NJ} N_{\text{ag}}}{C} \overline{M_{\text{u}}} \quad [27]$$

Two association steps models were tested for both D,12,12 (Fig. 12) and D,32,16 (Fig. 13). With two closed association steps, it was not possible to obtain good fits of the $M_{\text{wapp}} = f(C)$ curves. With the second model (co-operative formation of flower-like micelles followed by progressive intermicellar bridging), very good fits were obtained. Moreover, the aggregation numbers $N_{\text{ag}} = 20$ for D,12,12 and $N_{\text{ag}} = 15$ for D,32,16 obtained from those fits are consistent with the neutron scattering experiments and the results obtained in Ref. (26). Table 1 shows that calculated and experimental values of *CAC* are in good agreement.

In the case of D,32,16, as discussed above, the "flowers" are assumed to have a hydrodynamic radius of 150 Å. R_{H} can be calculated from [8] to [11], considering that "flowers" of D,32,16 are equivalent to micelles of $N_{\text{ag}} = 34$ unimers of one-half their molecular weight (i.e., 16,000). R_{H} of PEO 16,000 = 36.5 Å and the calculated values of "flowers" are 110 and 130 Å, respectively, for regular and polydisperse stars. As in the case of M,20,18, the best agreement is obtained with the polydisperse star model.

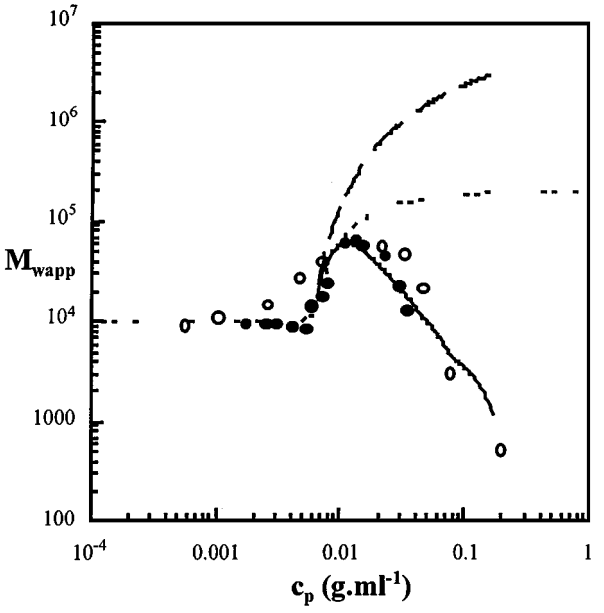

FIG. 12. Fit of the experimental $\overline{M_{wapp}} = f(C)$ curve of D,12,12 solution (○, Ref. 12; ●, this work) obtained with a two-step association model: (—, variation of $\overline{M_{wapp}}$; . . . , variation of molecular weight of the flowers $\overline{M_w}$; – –, variation of the total molecular weight of aggregates) $N_{ag} = 20$, $K_c = 10^{58}$, $K_0 = 10^5$, $2A_2 = 5 \times 10^{-4}$ ml mol g^{-2}, $3A_3 = 2.5 \times 10^{-2}$ ml^2 mol g^{-3}.

Remarks

The results were calculated with two virial coefficients, which may correspond to an oversimplification of the phenomenon at concentrations above "flower" overlapping. Nevertheless, the values of A_2 and A_3 are, as in the case of monofunctionalized PEO, lower than these found for pure PEO.

Even if some questions remain unresolved, one can give a description more detailed than those already proposed. The existence of a well-resolved peak in neutron scattering curves and its very low intensity at small angles indicate an homogeneous distribution of micelles in solution. The variation of the interparticular distance with c^a, with a close to 1/3, is also consistent with this homogeneity. If it was the case, viscosity divergence may be shown as described by Semenov *et al.* (30) as a consequence of "flower" overlapping, C_f^*.

One can evaluate C_f^* from the same arguments used to calculate C_m^* for monofunctionalized PEO, but the reference unimer corresponds to one-half of a chain: in other words, "flowers" are considered as being similar to micelles of monofunctionalized PEO but 2 times shorter. One obtains $[\eta] = 40.7$ and 73 ml g^{-1} respectively for D,12,12 and D,32,16. The calculated overlap concentrations of "flowers" C_f^* are 2.4×10^{-2} and 1.4×10^{-2} g ml^{-1}. These values are higher than $C_\eta = 1 \times 10^{-2}$ and 3×10^{-3} g ml^{-1} for D,12,12 and D,32,16, respectively. But they are very close to the concentrations at which an abrupt jump of viscosity was observed in another work and is reminiscent of Semenov *et al.*'s predictions (30). In our opinion, "flower" aggregation is a marginal phenomenon around concentrations C_η and C''. The fact that "flowers" have a higher intrinsic viscosity and hydrodynamic radius than unimers is enough to explain this initial viscosity divergence. Moreover, the two-step model corresponds to the formation of micelle aggregates, and one could assume that the distance between micelle centers inside aggregates is not concentration-dependent up to the point of aggregates overlapping, which is not observed in neutron scattering experiments.

The difference between the concentration dependencies of D between D,32,16 and D,12,12 or D,20,12 is related to the much lower *CAC* value in the first case. It is possible with D,32,16 to observe an increase in hydrodynamical radii due to "flower" aggregation prior to formation of an homogeneous system where interaction terms considerably affect D values. But, the first step of association, "flower" formation, is more easily observed in the latter two cases.

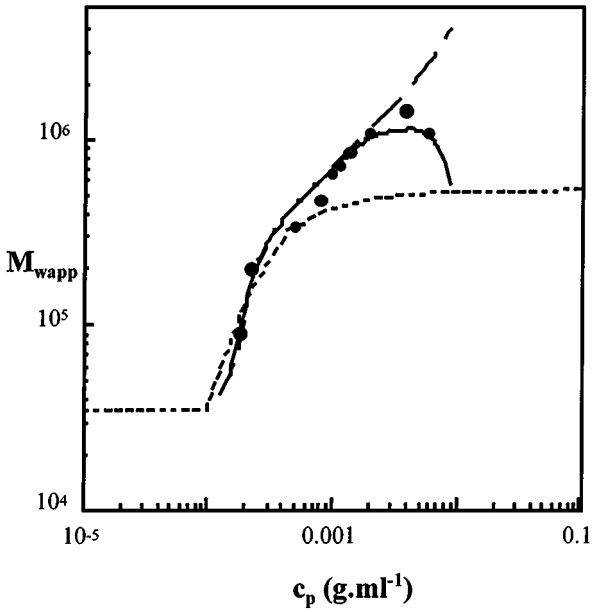

FIG. 13. Fit of the experimental $\overline{M_{wapp}} = f(C)$ curve of D,32,16 solution obtained with a two-step association model: (–, variation of $\overline{M_{wapp}}$; . . . , variation of molecular weight of "flowers" $\overline{M_w}$ a; – –, variation of the total molecular weight of aggregates) $N_{ag} = 15$, $K_c = 10^{73}$, $K_0 = 10^{5.8}$, $2A_2 = 1 \times 10^{-5}$ ml mol g^{-2}, $3A_3 = 0.02$ ml^2 mol g^{-3}.

CONCLUSION

This work gives a consistent description of the associative behavior of α-functionalized PEO. The co-operative formation of "flower-like" micelles readily explains various experimental observations: critical association concentration, indicated by fluorescence, static and dynamic light scattering, viscosity, and neutron scattering. A simple closed association model where aggregates of a given number of unimers are in equilibrium with free unimers is almost as satisfactory as a model of open association where micelle growth is limited by repulsion between long PEO chains. Rheological behaviors at higher concentrations,

i.e., much greater than that required for micelles overlapping, will be studied in more detail in a forthcoming paper.

For α,ω-functionalized PEO the most acceptable mechanism corresponds to a fast step of "flower" formation with a slower aggregation of "flowers," as was already qualitatively proposed. Nevertheless, the systematic comparison of information obtained from various experiments with samples of differing associativity has allowed a more precise description of these association steps.

For both types of polymer, it is interesting to note that polymer star models can give a good description of the micelles' and flowers' dimensions. We have shown that the increase in particle dimensions upon micellization also has an important effect on the concentration dependence of the system's viscosity. The most important change in viscosity does not correspond to the first divergence from linearity but is observed for much higher concentrations when all "flowers" overlap in a homogeneous system.

In fact, for samples with low associativity, *CAC* values are high and can be detected by light scattering experiments. Nevertheless, such systems become homogeneous just above *CAC* and it is difficult to follow further association steps. For samples with high associativities and very low *CAC*, micelles or "flower" formation cannot be detected by light scattering but progressive aggregate formation by "flower" bridging can be more easily followed.

REFERENCES

1. "Polymer in Aqueous Media, Performances through Association" (J. E. Glass, Ed.), Advances in Chemistry Series 223, Am. Chem. Soc., Washington, DC, 1989.
2. "Hydrophilic polymers. Performances and Environmental Acceptability" (J. E. Glass, Ed.), Advances in Chemistry Series 248, Am. Chem. Soc., Washington, DC, 1995.
3. Lundberg, D. J., Glass, J. E., and Eley, R. R., *J. Rheol.* **35**(6), 1255 (1991).
4. Kaczmarski, J. P., and Glass, J. E., *Macromolecules* **26,** 5146 (1993).
5. Alami, E., Rawiso, M., Isel, F., Beinert, G., Binana-Limbele, W., and François, J., *in* "Hydrophilic polymers. Performances and Environmental Acceptability" (J. E. Glass, Ed.), Advances in Chemistry Series 248, Chapter 18, Am. Chem. Soc., Washington, DC, 1995.
6. François, J., Maître, S., Rawiso, M., Sarazin, D., Beinert, G., and Isel, G., *Colloids Surf.* **112,** 251 (1996).
7. Maechling-Strasser, C., François, J., Clouet, F., and Tripette, C., *Polymer* **33,** 627 (1992).
8. Maechling-Strasser, C., Clouet, F., and François, J., *Polymer* **33,** 1021 (1992).
9. Nyström, B., Walderhaug, H., and Hansen, F. K., *J. Phys. Chem.* **97,** 7743 (1993).
10. Yekta, A., Xu, B., Duhamel, J., Adiwidjaja, H., and Winnik, M. A., *Macromolecules* **28,** 956 (1995).
11. (a) Chassenieux, C., Nicolai, T., and Durand, D., *Macromolecules* **30,** 4952 (1997); (b) Chassenieux, C., Johannsson, R., Durand, D., Nicolai, T., Vanhoorne, P., and Jérôme, R., *Colloids Surf. A* **112,** 155 (1996).
12. Oulyanova, N. N., Trabukina, E. B., Sabaneeva, N. V., Bykova, E. N., Kallistov, O. V., François, J., and Klenin, S. I., *Polym. Sci. Ser. A* **40,** 622 (1998).
13. Elias, H. G., *in* "Light Scattering from Polymer Solutions" (S. Huglin, Ed.), p. 428, Academic Press, London, 1972.
14. Maître, S., Ph.D. thesis, University Louis Pasteur, Strasbourg, France, 1997.
15. Kalyianafundaran, K., and Thomas, J. K., *J. Am. Chem. Soc.* **99,** 2039 (1977).
16. Turro, N. J., and Yekta, A. J., *J. Am. Chem. Soc.* **100,** 5951 (1978).
17. McNeil, R., and Thomas, J. K., *J. Colloid Interface Sci.* **83,** 57 (1981).
18. Denavand, K., and Selser, J. C., *Nature* **343,** 739 (1990).
19. Alami, E., Almgren, M., Brown, W., and François, J., *Macromolecules* **29,** 2229 (1996).
20. Raspaud, E., Lairez, D., and Adam, M., *Macromolecules* **27,** 2956 (1994).
21. Plestil, J., *Polymer* **31,** 2112, 2118 (1990).
22. Chassenieux, C., Nicolai, T., Durand, D., and François, J., *Macromolecules* **31,** 4035 (1998).
23. de Gennes, P.-G., "Scaling Concepts in Polymers Physics," Cornell Univ. Press, Ithaca, NY, 1979.
24. Doi, M., and Edwards, S. F., "The Theory of Polymer Dynamics," Clarendon Press, Oxford, 1986.
25. Edwards, S. F., *Proc. Phys. Soc. London* **88,** 265 (1966).
26. Beaudoin, E., and François, J., unpublished results.
27. Schmidt, M., and Burchard, W., *Macromolecules* **11,** 460 (1978).
28. Stockmayer, W. H., *Macromolecules* **13,** 580 (1980).
29. Tanford, C., *in* "Micellization, Solubilization, and microemulsions" (K. L. Mittal, Ed.), p. 119, Plenum, New York and London, 1977.
30. Semenov, A. N., Joanny, J. F., and Khokhlov, A. R., *Macromolecules* **288,** 1066 (1995).
31. Meguro, K., Takasawa, Y., Kawahashi, N., Tabata, Y., and Ueno, M., *J. Interface Sci.* **83**(1), 50 (1981).
32. Zimm, B. H., and Stockmayer, W. H., *J. Chem. Phys.* **17,** 130 (1949).
33. Stockmayer, W. H., and Fixmann, M., *Ann. N. Y. Acad. Sci.* **57,** 334 (1953).
34. Zimm, B. H., and Kilb, R. W., *J. Polym. Sci.* **37,** 19 (1959).
35. Louai, A., Pollet, G., Sarazin, D., François, J., and Moreaux, F., *Polymer* **32,** 703 (1991).